Optoelectronic and Thermoelectric Properties of the Tetragonal Structure of the Halide Perovskite Material RbSeBr3 used for low-cost Photovoltaic

Rabah Mehyaoui and Karima Benyahia

Abstract− Perovskite solar cells are the future of energy production due to the high- efficiency and low production costs. In this work, the structural, electronic and optical properties of the tetragonal inorganic halideperovskiteRbSeBr3 are performed using the full potential linearized augmented plane waves (FP-LAPW) method with the PerdewBurke–Ernzerh generalized gradient approximation (PBE-GGA) as well as the local density approximation (LDA) and the modified Becke-Johnson (mBJ-LDA) as exchange correlation potentials using Wien2k code. Furthermore, the thermoelectric propertieshave been calculated using BoltzTrap code, the obtained results show that the studied compound (RbSeBr3) has a metallic character and can be used as an absorber in UV-interval; on the other hand the thermoelectric power reveals a high value.

***Keywords*: Electronic and Optical properties, Inorganic halideperovskite, Tetragonal RbSeBr3,FP-LAPW,PBE-GGA,LDA,mBJ-LDA,Wien2k,Thermoelectric properties, BoltzTrap.**

NOMENCLATURE

FPLAPW	Full potential Linearized augmented plane wave
PBE-GGA	Perdew–Burke–Ernzerh generalized gradient approximation.
LDA	Local density approximation.
mBJ-LDA	Modified Becke-Johnson LDA.

I. INTRODUCTION

Solar energy is one of the most accessible, cost-effective, and environmentally friendly sources of energy in the world, yet in most locations, the costs associated with harvesting solar energy using traditional photovoltaic's (PVs) are still expensive compared toconventional fossil-fuel energy sources[1,2].

Therefore, it is essential to create next-generation PVs that are both affordable and efficient. Perovskite solar cells (PSCs), a novel thinfilm PVs technology, have just come to attract more attention and research [3, 4]. The power conversion efficiency (PCE) according to Kojima et al. has quickly increased from 3.8% in a short amount of timein 2009 to a verified 22.1% in 2017[5-6].

The term perovskite originally refers to the mineral calcium titanate with the chemical formula CaTiO3 [7], which has a very important structure, it is the basis of the definition of a Perovskite [8];this mineral specie was discovered in Russia by the German G. Rose in 1839. The first studies on perovskiteshave been concentrated on titanate compounds' structure and biaxial optical characteristics [7]. The ideal perovskitestructure has a cubic unit cell and the general formula ABX_3.The A cation, B cation, and X anion are all positioned in the body's center, the structure is symmetrical in the Oh direction. The perovskite structure was described by V. Goldschmidt in 1926 [9]who studied a large number of synthetic perovskite compounds with different compositions. These compounds were initially employed as pigments in paints and other coatings, in addition to their importance in fundamental research[10]. Electronic properties of perovskites aroused more interest from the mid-1940s, when the ferroelectricity in BaTiO3 perovskite has been demonstrated [11, 12].

The perovskite RbSeBr3 crystallizes in the tetragonal P4mm space group. Rb is bound to twelve Br atoms to create RbBr12 cuboctahedra, which share corners with corresponding RbBr12 cuboctahedra of twelve, faces [13].In this study, we have simply taken into account the tetragonal structure of RbSeBr3 utilizing PBE-GGA to study its unexplored structural, electronic, optical, and thermoelectric properties. The paper is organized as fellows: Part.1 supplies an introduction, Part 2 includes computational details, Part 3 covers the results and we finish with a conclusion

II. COMPUTATIONAL METHODOLOGIES

All calculations in this study were completed using the WIEN2K code's and the implementation of the full-potential linear augmented plane wave (FP-LAPW) method within the confines of density functional theory (DFT) [14,15]. In order to evaluate the prior properties, Perdew-Burke-Ernzerh generalized gradient approximation (PBE-GGA) was used for the calculations [16] as well as the local density approximation (LDA) [17] and modified Becke-Johnson (mBJ-LDA) [18]. A linear combination of the radial Schrödinger equation solution times the spherical harmonic is used in the interstitial region, along with the plane wave basis set. For the tetragonal structure (P4mm space group) the RMT value is 2.5 a.u for the atoms Rb: [Kr] 5s1, Se:[Ar] 3d104s24p4 and Br:[Ar] 3d104s24p5. To expand the wave functions in the interstitial region, we took the value of Kmax =10000. The $R_{mt} * K_{MAX}$ is taken equal to 7 (where k_{max} is the plane wavescutoff) [19]. In the muffintin spheres, the angular momentum expansion is taken into account up to

Manuscript received October 25, 2022; revised July 7, 2023.

R. Mehyaoui and K. Benyahia are with Materials Science and Applications Laboratory (LSMA), BelhadjBouchaib University, AinTemouchent, ALGERIA. (E-mails: rabah.mehyaoui@univ-temouchent.edu.dz, karima.benyahia@univ-temouchent.edu.dz).

Digital Object Identifier (DOI): 10.53907/enpesj.v3i1.172

lmax = 10. All computations are carried out in a k-mesh with 21 × 21 × 21 k pointsin the irreducible Brillouin zone.

III. RESULTS AND DISCUSSIONS

1. GEOMETRICAL STRUCTURE AND ITS PROPERTIES

As previously stated, the RbSeBr3's tetragonal structure, which is seen in Fig. 1, has been taken into account and optimized. The structure belongs to the P4mm space group [20].

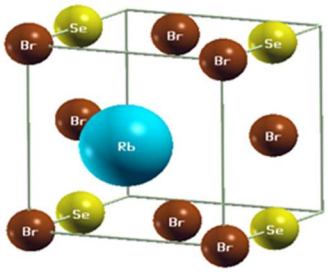

Fig. 1. Tetragonal Structure of RbSeBr3

To plot the evolution of the total energy as a function of the volume, we used the Murnaghan Equations [21]:

$$E(V) = E_0 + \frac{B_0}{B'(B'-1)}\left[V\left(\frac{V_0}{V}\right)^{B'} - V_0\right] + \frac{B_0}{B'}(V - V_0)$$

$$B_0 = V\frac{\partial^2 E}{\partial V^2}$$

$$V = V_0\left(1 + \frac{B'P}{B_0}\right)^{-1/B'}$$

Where, V_0 is the reference volume, V is the warped volume, B_0 is the bulk modulus, and B′ is its derivative. E_0 is the reached minimum ground state energy [21].

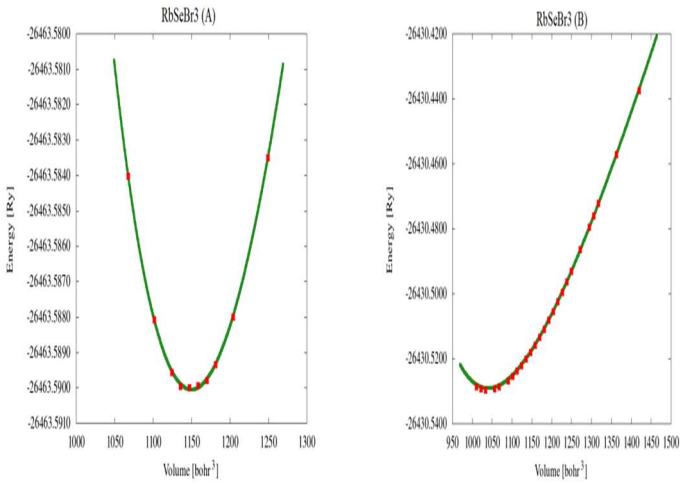

Fig. 2. The variation of the total energy of the tetragonal structure of RbSeBr3 for:A) GGA B) LDA approximations depending on the volume

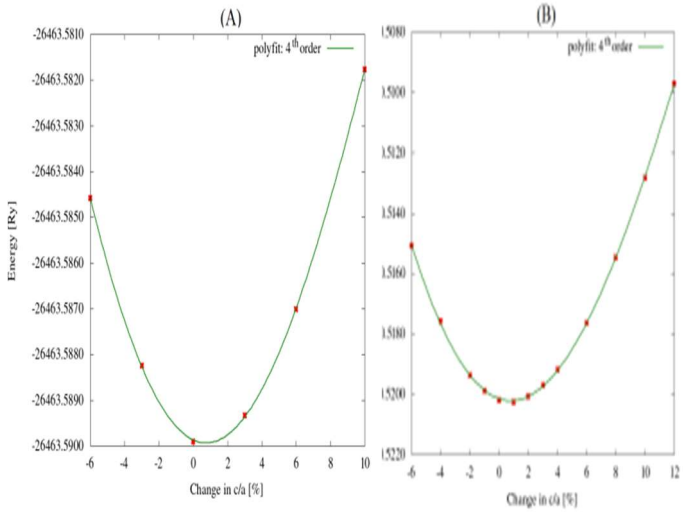

Fig. 3. The variation of C/A ratio of the tetragonal structure of RbSeBr3 for: A) GGA, B) LDA Approximations with constant volume.

The compounds' ground state minimum energy and optimal volumes are determined from the Figures (2-3). Table I includes the equilibrium parameters, bulk modulus and its derivative, volume, gap energy, and total energies. They agree well with other theoretical calculations [20].

2. ELECTRONIC PROPERTIES

2.1 THE ELECTRONIC BAND STRUCTURE

The band structures for spin-up and spin-down shown in Fig. 4 are computed using the GGA-PBE exchange correlation functionals in order to explore the electronic properties. For this purpose, the high symmetry path of the k-points inside the Brillouin zone taken into account is Γ → X → M → Γ →Z → R → A → Z→ X→ R→ M→ A. From the band structures, the absence of a forbidden band indicates the metallic character of the studied material. The A point containsboth the valence band maximum (VBM) and the conduction band minimum (CBM).

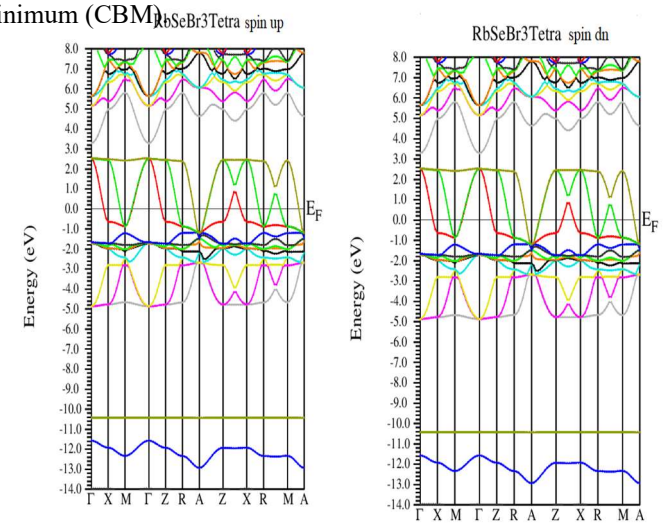

Fig. 4. Band structure of RbSeBr3 for GGA-PBE Approximation.

Table. I

Lattice parameters (A_o), Bulk modulus B_0(GPa) and its derivative B', Total energy (Ry), Fermi energy (Ry) and GAP energy (eV) of the tetragonal structure of RbSnBr3 using GGA, LDA and mBJ -LDA approximations.

Tetragonal structure		a(A°)	b(A°)	c(A°)	V_0(a-u)3	B_0(GPa)	B '	E(Ry)	E_F(Ry)	Eg(eV)
Murnaghan	GGA	5.458	5.458	5.696	1150.115	26.134	4.587	26463.590	0.0545	0
	LDA	5.364	5.359	5.226	1040.719	37.580	5.953	26430.529	0.2245	0
mBJ -LDA		/	/	/	/	/	/	/	0.2649	0
Other work [20]		5.523	5.523	5.518	1135.853	/	/	/	/	0

Table. II

SPIN MAGNETIC MOMENTS OF MIXED CHARGE DENSITY

INTERSTITIAL	0.00037
Rb	0.00033
Se	0.00367
Br(1a)	-0.00177
Br(2c)	-0.00024
CELL	0.00060

2.2 THE DENSITY OF STATES

To gain insight into how the various atoms and their orbitals contribute to the curves in band structures, we estimated the total density of states (TDOS) and partial density of states (PDOS) for the tetragonal structure of RbSeBr3. The TDOS plots shown in Fig. 5 reveal a strong contribution of p-state of the atoms (Se, Br) along the borders of the Fermi level for both spins Up/Dn. The valence band (VB) is dominated by the p-state of the atoms (Se, Br), while the conduction band is characterized by a high contribution of Rb-d states. We notice a low contribution of s states in both bands and the Fermi level is characterized by a high hybridization of Se-p states and Br-p states leading to a metallic character of RbSeBr3 in the tetragonal structure.

3. OPTICAL PROPERTIES

In this work, we examined the real $\varepsilon_1(\omega)$ and imaginary $\varepsilon_2(\omega)$ components of the dielectric constant given by Eq.4 in the energy range(0 – 14)eV. Both components are shown in Fig. 6. the extinction coefficient k(ω), the electron energy loss spectra (EELS) L(ω), the reflectivity R(ω), the optical conductivity σ(ω), the absorption coefficientα(ω), and the refractive index n(ω) are displayed in Figures (7,8). These properties, which depend on frequencies and are derived from the complex dielectric function, stated in Eq.4, they are in fact frequency-dependent [23–24].

$$\varepsilon(\omega) = \varepsilon_1(\omega) + i\,\varepsilon_2(\omega) \tag{4}$$

$$n(\omega) = \left(\sqrt{\varepsilon_1(\omega)^2 + \varepsilon_2(\omega)^2} + \varepsilon_1(\omega)\right)^{1/2} \tag{5}$$

$$k(\omega) = \left(\sqrt{\varepsilon_1(\omega)^2 + \varepsilon_2(\omega)^2} - \varepsilon_1(\omega)\right)^{1/2} \tag{6}$$

$$R(E) = \frac{(n-1)^2 + k^2}{(n+1)^2 + k^2} \tag{7}$$

$$L(\omega) = \frac{\varepsilon_2(\omega)}{\varepsilon_1(\omega)^2 + \varepsilon_2(\omega)^2} \tag{8}$$

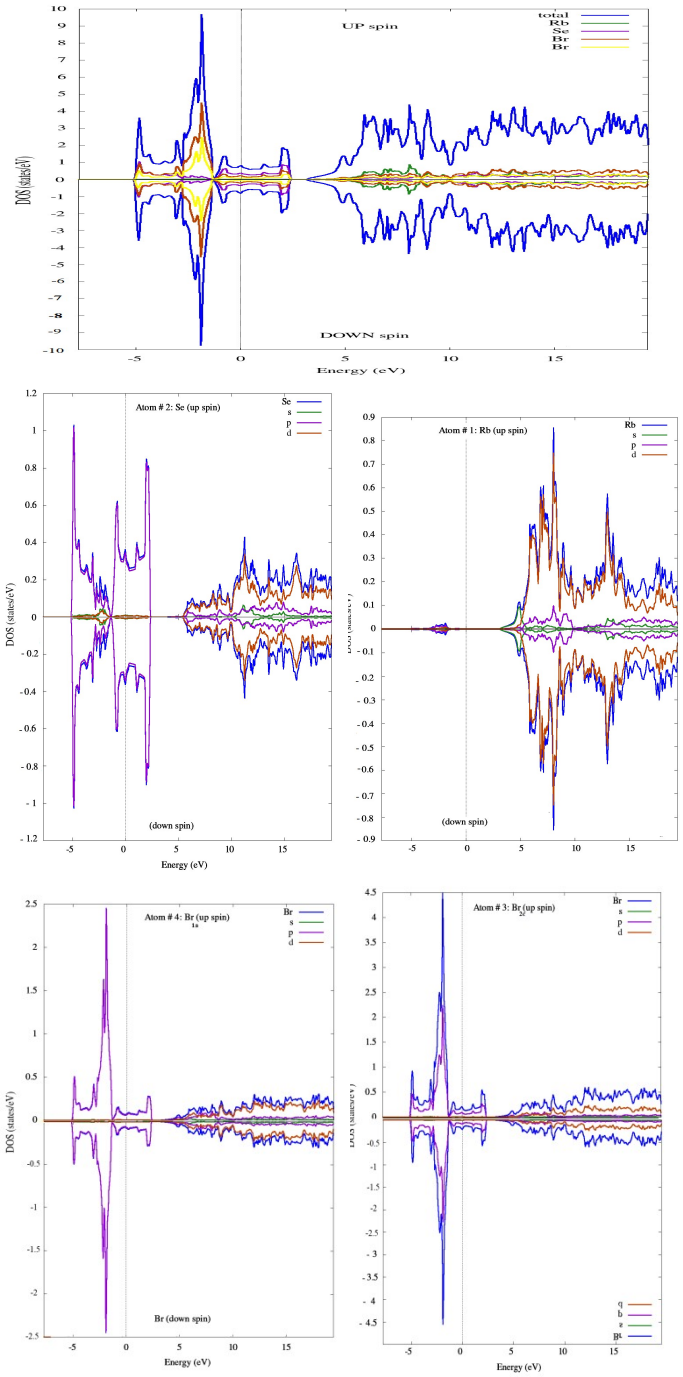

Fig. 5. Total and partial density of state for the tetragonal RbSeBr3

All of the previous properties actually depend only on the components of the dielectric function at specific frequencies which is used to determine the optical properties [25, 26]. The equations Eq. 5–8 are used to obtain their expressions. [24].

Both the electronic polarizability properties of perovskite and the scattering behavior of electromagnetic (EM) radiation incident on perovskite are explained by the curve of the real component of the dielectric function in Fig. 6 related to perovskite photon energy compound [27]. At zero energy of $\varepsilon_1(0)$, the static permittivity is -2200 along yy and -350 along xx and zz. It is clear that the value of $\varepsilon_1(\omega)$ varies from visible to UV zone (1.7 to 12 eV). Increasing and tending to zero suggest that it behaves like a metal in this region. Inside a metallic conductor, there is no electric field because the free charge remains on the surface of the metal, and a significant plasmonic excitation exists and can survive.

The response of a connection to (EM) radiation is given by the imaginary part of the dielectric function, as shown. 6. This indicates the state transition that occurs from the valence band to the conduction band [27, 28]. We find that $\varepsilon_2(0)$ is equal to 16050 along yy and 7000 along xx and zz. After that, this value starts to decrease and approaches zero.

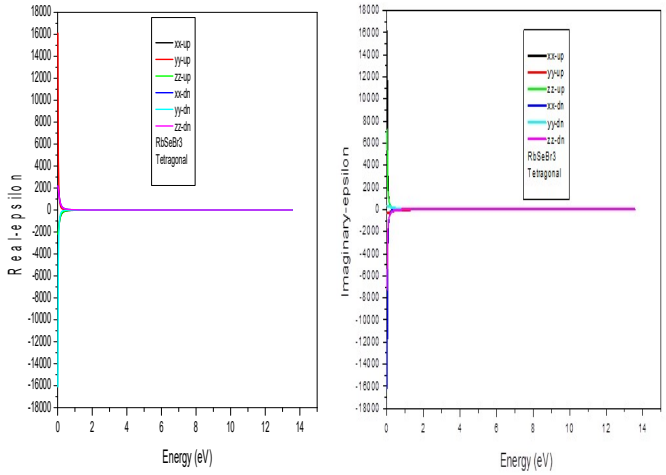

Fig.6. Real $\varepsilon_1(\omega)$ and imaginary$\varepsilon_2(\omega)$ components of dielectric constant of RbSeBr3.

Figure 7(A) shows the absorption coefficient α(ω) of RbSeBr3 perovskite, showing how the incident light is absorbed. It also provides information on the degradation of the outgoing light as it passes through the material, showing how EM radiation is attenuated [24, 27]. The value of α(ω) approaches zero in the range 0 to 1.5 eV. The halide perovskite is nearly optically transparent in these regions because no light absorption occurs. As a result, this compound has negligible absorption in this range. Absorption at (2.8, 7.8, and 11eV) demonstrates the effectiveness of this material in the UV range. This result demonstrates that RbSeBr3 can be incorporated into sensitive devices as a UV absorber to effectively protect against harmful UV radiation. In contrast, fig. 7 (B) displays the plot of real and imaginary optical conductivity that almost matches the absorption spectra α(ω) in the UV region.

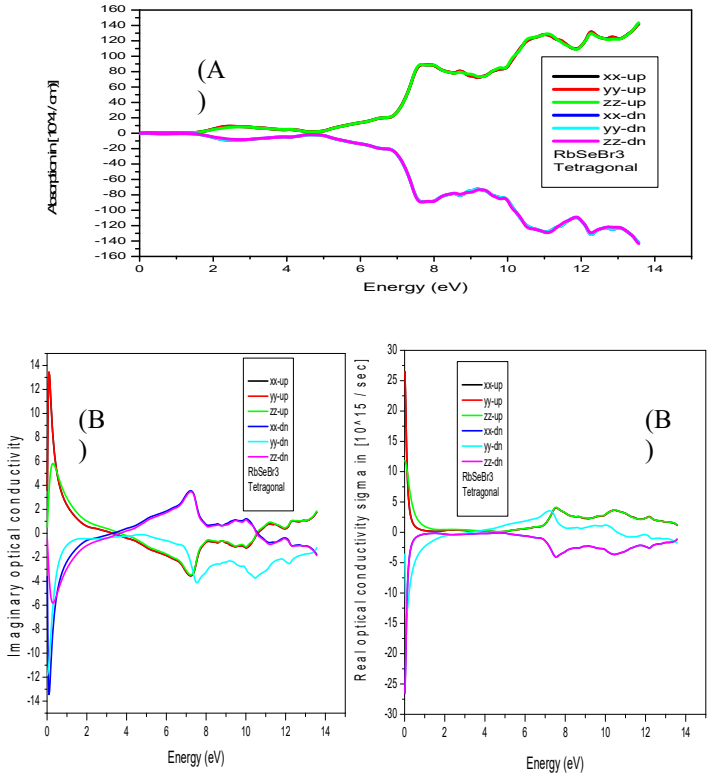

Fig. 7. (A) absorption spectra α (ω), (B) Real and Imaginary optical conductivity of RbSeBr3.

The following expression in Eq. 9 sheds light on how an EM beams or light moves through a compound.

$$N(\omega) = n(\omega) + i\,k(\omega) \quad (9)$$

n(ω) represents the absolute refractive index and k(ω) represents the extinction coefficient. Figure 8 (A) shows the n(ω) curves. It details how much incident light is refracted or bent on its way through the material [28,29].
The maximum at 0 eV is 85 along yy and 58 along xx and zz axes, and then decreases to almost 0 in both visible and ultraviolet.
The values of the extinction coefficient k(ω) in Fig.8(B) provide information regarding the propagation depth of the EM wave's emergent photons as they move through the compound. The graph indicates that the k(0) value is 95 alog yy and 63 alongxx and zz axes, and then in the visible and UV sections it is almost lining with the previous graph. Fig. 8(C) illustrates how an incident EM beam causes the loss of energy of electrons in a compound. We can learn about the plasmonic excitations from the L(ω) spectra [30], from which we infer that the energy loss truly results from electronic excitations. The EELS plot reveals that the UV zone, where it reaches the largest peak of the compound, contains the majority of the losses. Next, we estimated the reflectivity R(ω) spectra, which are displayed in Fig. 8 (D), where we can see that the reflectivity decreases in the visible region and then increases as the energy level rises in the UV interval.

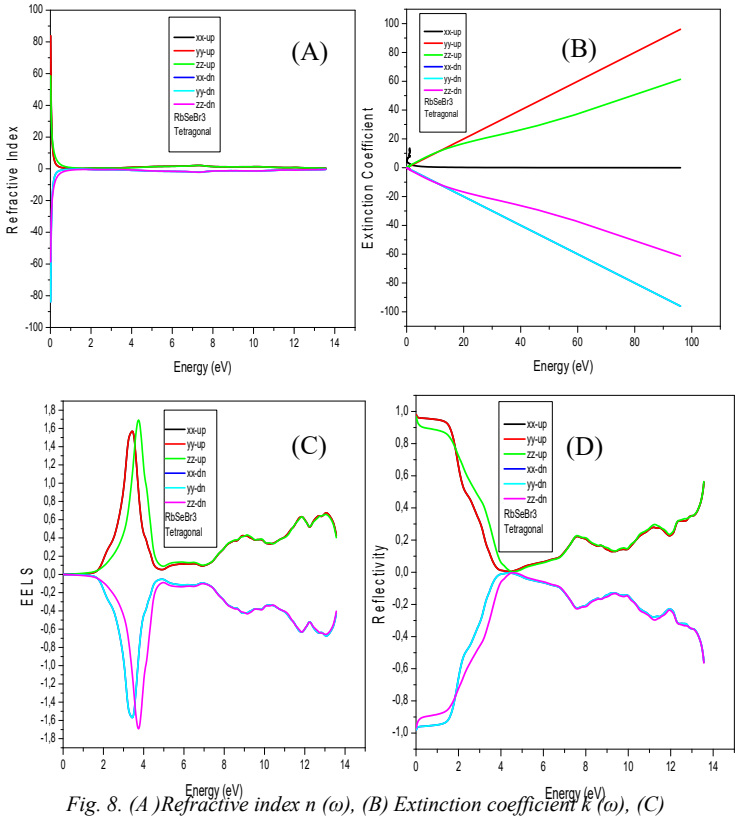

Fig. 8. (A)Refractive index n (ω), (B) Extinction coefficient k (ω), (C) Electron energy loss function L (ω) and (D) Reflectivity R (ω) of RbSeBr3.

4. THERMOELECTRIC PROPERTIES

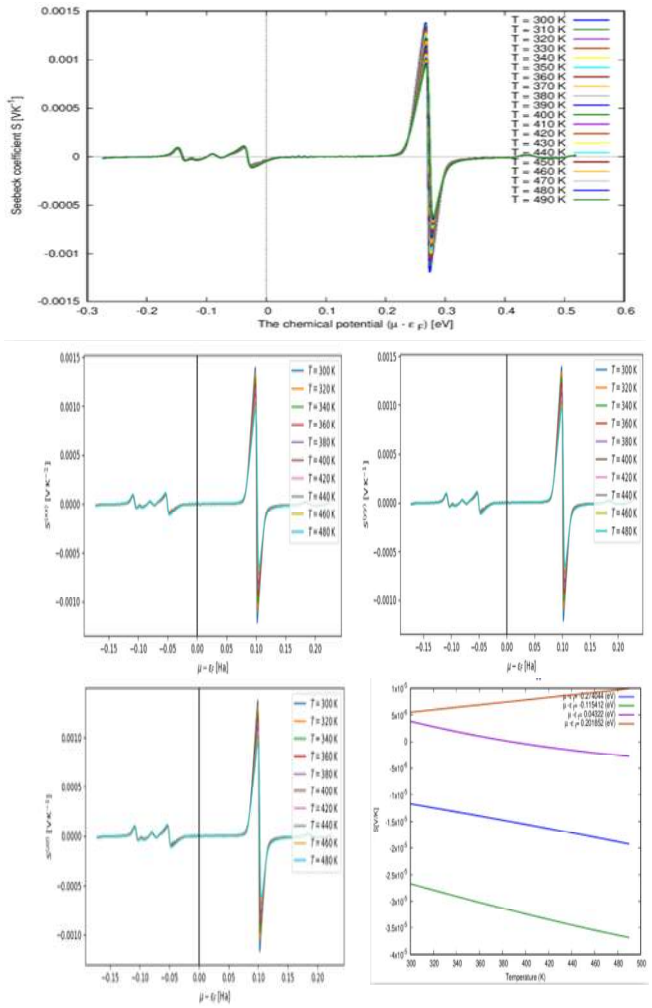

Fig.9. Seebeck coefficient of RbSeBr3

Finally, the thermoelectric (TE) properties Seebeck coefficient (S), electrical conductivity per relaxation time (σ/τ), and power factor (PF) were investigated. These were calculated based on chemical potentials (μ) in the energy range 0.25–0.5 eV at temperatures between 300–500 K.

The magnitude of the thermoelectric voltage caused by the temperature difference in the connection is described by the Seebeck coefficient (S). The nature of the dominant carrier is indicated by the letter S [22]. The largest peak of S occurs at 14 mV/K, 0.25 eV at a temperature of 300 K, and the peak value of S varies with temperature. Figure 9 shows the variation of S with chemical potential and temperature along the xx, yy and zz axes.

Figure 10 shows the conductivity per relaxation time (σ/τ) as a function of μ. This metric provides information on the electrical conductivity of a material produced by the flow of electrons along a temperature gradient from hot to cold. From the peak values of σ/τ plotted against μ, it can be observed that they do not change significantly with temperature. The highest value is ~ 6.2 Ω/ms at 300K.

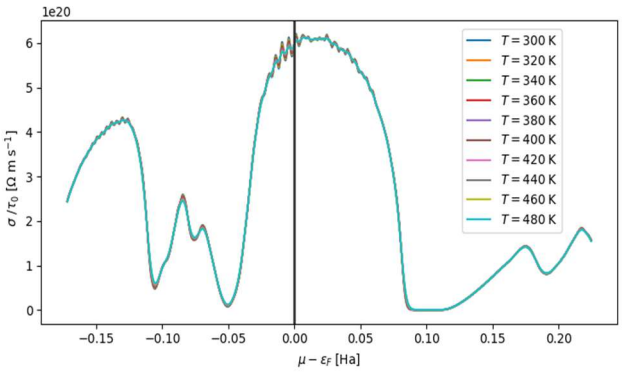

Fig.10. *The* electrical conductivity per relaxation time (σ/τ) as a function of μ of RbSeBr3

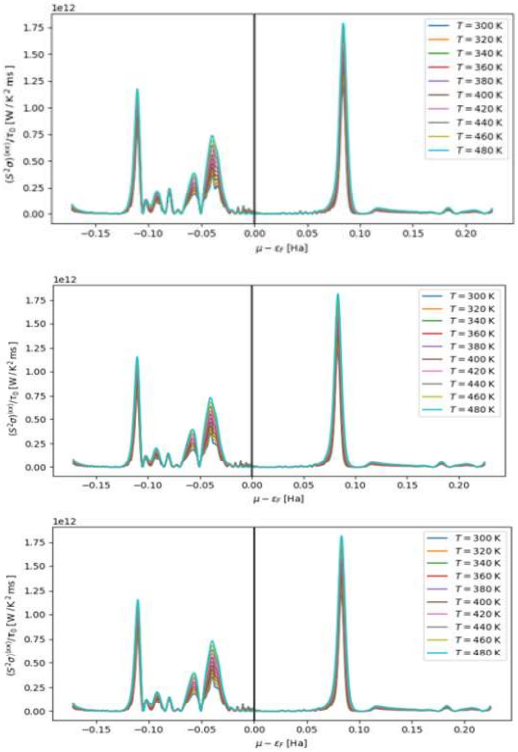

Fig.11. Power Factor of the Tetragonal RbSeBr3

The material's power factor (P.F.) is a crucial indicator of how effective its thermoelectric properties are. The feature is directly dependent on the Seebeck coefficient and electrical conductivity, as seen by the expression P.F = S2σ/τ [22]. The plots of P.F. with respect to μ are presented in Fig. 11. From 300 K to 500 K, the power factor increases, reaching a high value of 1.8 W/K2ms at 0.8 Ha at 480 K.

IV. CONCLUSION

The halide perovskite RbSeBr3 reported in this work was ultimately explored to establish its structural, electronic, optical, and thermoelectric properties using the FP-LAPW method. The findings indicate that RbSeBr3 lacks an energy band gap and behaves like a metal. Indeed, the Fermi level is dominated by a high hybridization of Se-p states and Br-p states. The high absorption peaks at (2.8, 7.8, and 11eV) demonstrate the effectiveness of this material in the UV range. It is considered as an absorber in the UV range and can be used in sensitive devices to protect against harmful UV radiation. Furthermore, the investigated thermoelectric properties suggest using RbSeBr3 as appropriate for thermoelectric power generators.

REFERENCES

[1] Gratzel, M. (2014). The light and shade of perovskite solar cells. Nat. Mater. 13, 838–842.

[2] Green, M.A., Ho-Baillie, A., and Snaith, H.J. (2014). The emergence of perovskite solar cells. Nat. Photon. 8, 506.

[3] Liu, M., Johnston, M.B., and Snaith, H.J. (2013). Efficient planar heterojunctionperovskite solar cells by vapourdeposition. Nature 501, 395.

[4] Correa-Baena, J.P., Saliba, M., Buonassisi, T., Gratzel, M., Abate, A., Tress, W., and Hagfeldt, A. (2017). Promises and challenges of perovskite solar cells. Science 358, 739–744.

[5] Kojima, A., Teshima, K., Shirai, Y., and Miyasaka, T. (2009). Organometal halide perovskites as visible-light sensitizers for photovoltaic cells.J.Am. Chem. Soc. 131, 6050–6051.

[6] National Center for Photovoltaics, Best Research-Cell Efficiencies, National Renewable Energy Laboratory, https://www.nrel.gov/pv/assets/images/efficiencychart.png.

[7] H. L. Bowman, On the structure of perovskite from the burgumer Alp, Pfitschthal, Tyrol.Mineral. Mag. 1908, 15, 156–176

[8] H. F. Kay and P. C. Bailey. "Structure and Properties of CaTiO3".ActaCryst. (1957), 10, 219

[9] V. M. Goldschmidt, Die Gesetze der Krystallochemie. Naturwissenschaften 1926, 14, 477–485

[10] V. M. Goldschmidt, Titanium pigment and process of producing the same. 1922.

[11] E. Wainer, High titania dielectrics. J. Electrochem. Soc. 1946, 89, 331–356

[12] R. Miyake .and S. Ueda, On polymorphic change of BaTiO3. J. Phys. Soc. Jpn. 1946, 1, 32–33

[13] The Materials Project , 36 MATERIALS SCIENCE , LBNL United States, (2020).

[14] P. Blaha, K. Schwarz, G. K. H. Madsen, D. K vasnicka, and J.itz,wien2k, An Augmented Plane Wave Plus Local Orbitals Program for Calculating Crystal properties (Vienna University of Technology, Vienna,Austria, 2001).

[15] W. Kohn and L. J. Sham, Phys. Rev. A 1133, 140, 1965.

[16] K. Schwarz and P. Blaha, "Solid state calculations using WIEN2k," Comput.Mater. Sci., vol. 28, no. 2, pp. 259–273, 2003

[17] J.P. Perdew, Y. Wang , Phys. Rev. B 1992;45:13244

[18] F. Tran, P. Blaha, Phys. Rev. Lett. 102 (2009), 226401.

[19] P. Blaha, K. Schwarz, G. Madsen, D. Kvasnicka, J. Luitz, An Augmented PlaneWave Plus Local Orbitals Program for Calculating crystals Properties..(2008)

[20] J. Anubhav, O. S. Ping, H. Geoffroy, C. Wei, Richards, W. Davidson, D. Stephen, C. Shreyas, G. Dan , S. David and C. Gerbrand, P. Kristin. APL Materials, p. 011002. 1, 2013.

[21] F. D. Murnaghan, "The Compressibility of Media under Extreme Pressures," Proceedings of the National Academy of Sciences of the USA, Vol. 30, No. 9, 1944, pp. 244-247.

[22] R. Sharma, A. Dey, S. A. Dar and V. Srivastava, A DFT investigation of CsMgX3, India (2021).

[23] G.J. Snyder, E.S. Toberer, Nat. Mater. 7 (2008) 105.

[24] V Kumar, A Dey, S Thomas, M.A. Zaeem, D.R Roy, Phys. Chem. Chem. Phys. 23 (2021) 10409–10417.

[25] J. Bechhoefer, Kramers–kronig, bode, and the meaning of zero, Am. J. Phys. 79(2011) 1053–1059.

[26] C.C. Kim, J. Garland, P. Raccah, Modeling the optical dielectric function of thealloy system Al x Ga 1- x as, Phys. Rev. B 47 (1993) 1876.

[27] S.A. Dar, R. Sharma, V. Srivastava, U.K. Sakalle, RSC Adv. 9 (2019) 9522.

[28] V Kumar, A Dey, S Thomas, M.A. Zaeem, D.R Roy, Phys. Chem. Chem. Phys. 23 (2021) 10409–10417.

[29] H.M. Ghaithan, Z.A. Alahmed, S.M.H. Qaid, M. Hezam, A.S. Aldwayyan, ACS Omega 5 (2020) 7468.

[30] G.J. Snyder, E.S. Toberer, Nat. Mater. 7 (2008) 105.

Rabah Mehyaoui was born on 16/12/1998 in Sidi Bel Abbes, ALGERIA. Graduated as a secondary school teacher (PES) field: Physics from ENS Taleb Abderrahmane, Laghouat, ALGERIA. Also a Master degree in: materials Physics from Djillali Liabes University, Sidi Bel Abbes, ALGERIA. Currently working as a high school teacher in Sidi Bel Abbes, Algeria, and a PHD student within the Materials Science and Applications Laboratory (LSMA) at the University of Ain Temouchent, Belhadj Bouchaib, AinTemouchent, Algeria.